Time Effects Relate to Crushing in Sand

Article *in* Journal of Geotechnical and Geoenvironmental Engineering · September 2010

DOI: 10.1061/(ASCE)GT.1943-5606.0000335

2 authors:

Hamid Karimpour
Stantec
7 PUBLICATIONS **177** CITATIONS
SEE PROFILE

Poul V. Lade
George Mason University
212 PUBLICATIONS **9,623** CITATIONS
SEE PROFILE

Time Effects Relate to Crushing in Sand

Hamid Karimpour[1] and Poul V. Lade, M.ASCE[2]

Abstract: Based on previously obtained experimental results, a mechanistic picture of time effects in granular materials is presented. Accordingly, time effects are caused by grain crushing, which in turn is time dependent, as indicated by static fatigue of brittle materials. Triaxial compression tests have been performed on Virginia Beach sand at high pressures, where grain crushing is prevalent, to study effects of initial loading strain rates on subsequent amounts of creep and stress relaxation. Grain size distribution curves were determined after each test and the amount of crushing, as characterized by Hardin's breakage factor, is related to the energy input to the triaxial specimens. A pattern emerges that indicates the importance of crushing for the axial and volumetric strains, while rearrangement and frictional sliding between intact grains play much smaller roles in the stress-strain and volume change behaviors of granular materials at high stresses and shear strains. Because particle crushing is a time-dependent phenomenon described as static fatigue or delayed fracture, the close relation between time effects and crushing in granular materials is established.

DOI: 10.1061/(ASCE)GT.1943-5606.0000335

CE Database subject headings: Creep; Granular media; Sand; Material; Soil properties; Strain rates; Time dependence; Triaxial tests.

Author keywords: Creep; Crushing; Granular materials; Sand; Soil properties; Strain rate; Time dependence; Triaxial tests.

Introduction

Geotechnical structures such as embankments, bridge abutments, retaining structures, slopes, etc., have been observed to deform and settle with time. Long-term deformations may cause these structures to distort and fail. Time effects in clay, other than consolidation, usually follow a classic viscous type of behavior referred to "isotach" behavior (Suklje 1969; Tatsuoka et al. 2000). This means that a unique stress-strain–strain-rate relation exists for clays. Sand, however, does not obey this classic viscous behavior and is termed "nonisotach" (Tatsuoka et al. 2000; Augustesen et al. 2004).

Recent studies (Lade and Liu 1998; Lade 2007; Lade et al. 2009, 2010) have indicated that time effects in sand are controlled by crushing of particles. However, grain size distributions were not determined after the experiments to prove the direct connection in these studies. One study was conducted on fine Antelope Valley sand (Lade and Liu 1998, Lade 2007), a relatively friable sand obtained from a streambed in the desert north of Los Angeles. The results of this study are summarized in Fig. 1 in which a comparison is made between creep and stress relaxation after one day. The points of initiation of creep have been located on the base curve, and the end points obtained after approximately one day of creep are shown relative to the initiation points. These end points define a consistent stress-strain relation. Similarly, a consistent stress-strain relation is obtained following one day of stress relaxation. It is clear that the amount of creep and the amount of relaxation resulting after one day define curves that are located at quite different positions. While crushing was evident from the grain sizes that came out of the specimens after testing, the sand was so friable that obtaining reliable grain size distributions after the experiments was questionable because they would be determined from sieve analyses involving shaking a stack of sieves which could easily cause additional particle crushing.

In the other study (Lade et al. 2009, 2010) experiments were performed on crushed coral sand. Fig. 2 shows a similar comparison between stress-strain relations after one day of creep and approximately one day of stress relaxation. It is again clear that the amount of creep and the amount of relaxation define curves that are located at quite different positions. The consistency of the granular material after testing was that of a paste whose grain size distribution would also be difficult to determine accurately. Each of these studies was performed at conventional geotechnical pressures at which crushing occurred in both sands.

Because the real proof that crushing is related to all aspects of time effects was missing from these studies, the investigation presented here was performed on conventional beach sand consisting of much stronger quartz and feldspar particles with definite grain size distributions determined before and after each experiment. Negligible time effects and very little crushing are observed in beach sand at conventional geotechnical pressures. It was therefore necessary to perform all experiments at elevated pressures where time effects and crushing are more evident. The testing program therefore consisted of repeating some of the previous experiments on beach sand to study strain rate effects, creep, and stress relaxation and with determination of grain size distribution curves before and after the experiments. Included is also a study of the effect of the initial loading strain rate on the subsequent amounts of creep and stress relaxation.

It has previously been observed that particle crushing is related to energy input per unit volume of material (including energy contributions from both shear strains and volumetric strains)

[1]Graduate Student, Dept. of Civil Engineering, Catholic Univ. of America, Washington, DC 20064.

[2]Professor, Dept. of Civil Engineering, Catholic Univ. of America, Washington, DC 20064 (corresponding author). E-mail: Lade@cua.edu

Note. This manuscript was submitted on August 18, 2009; approved on February 3, 2010; published online on August 13, 2010. Discussion period open until February 1, 2011; separate discussions must be submitted for individual papers. This paper is part of the ***Journal of Geotechnical and Geoenvironmental Engineering***, Vol. 136, No. 9, September 1, 2010. ©ASCE, ISSN 1090-0241/2010/9-1209–1219/$25.00.

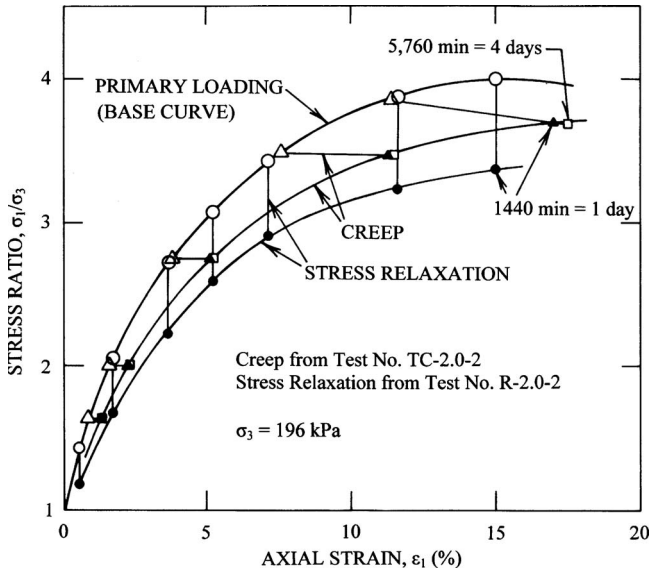

Fig. 1. Comparison of creep and stress relaxation experiments performed in two triaxial compression tests on Antelope Valley sand

(Lade et al. 1996). Comparison of creep and stress relaxation will therefore be based on initiation of these phenomena at points that have reached the same amount of energy input/volume. Other options would be to initiate creep or stress relaxation from the same deviator stress or the same axial strain. However, using energy input/volume as basis for comparisons is the option that seems most consistent because energy input/volume includes both stresses and strains in determination of common points from which to make the comparisons.

It should be emphasized that crushing is an important effect that can occur at low pressures for weaker granular materials or at high pressures common in geotechnical applications such as pile driving and blasting near the bottom of deep wells and near deep

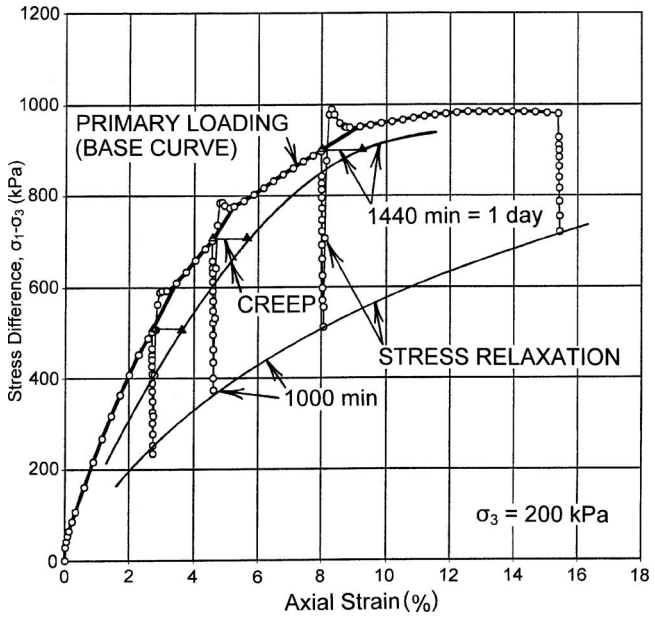

Fig. 2. Comparison of creep and stress relaxation experiments performed in two triaxial compression tests on crushed coral sand

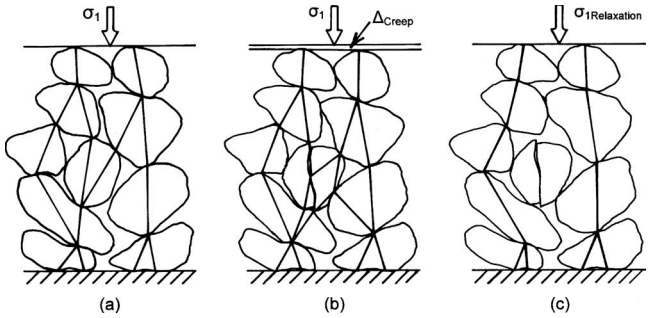

Fig. 3. (a) Initial force chains in particle structure and effects of grain crushing in (b) creep test and in (c) stress relaxation test

tunnels. Therefore, time effects can occur in granular materials under any circumstance where particle crushing is possible.

Previous Studies

Creep, relaxation, and strain rate effects are well-known time effects in granular materials. Comprehensive reviews of time-dependent behavior of soils and models for characterization of this behavior have recently been presented in the literature (Augustesen et al. 2004; Liingaard et al. 2004). The essence of these reviews is that clay and sand behave differently with respect to time. Additional review and explanation of time effects in sands were presented by Lade et al. (2009, 2010).

Based on the studies by Lade et al. (2009, 2010), a mechanistic picture of time effects in sand was proposed. This picture involves particle breakage with time. Particle breakage may not occur and time effects are negligible in granular materials at very low stresses. Time effects become significant with increasing confining pressure and increasing stress difference, as has been observed in several studies (Yamamuro and Lade 1993; Yamamuro et al. 1996; Lade et al. 1996). These studies also noted the association between particle crushing and its occurrence with time.

Single particle breakage and breakage of particles in assemblies have been the subject of many studies, both experimental and numerical, as exemplified by those performed by McDowell and Bolton (1998), Nakata et al. (1999, 2001a,b), Tang et al. (2001), Kou et al. (2001), Cheng et al. (2003), Coop et al. (2004), Lobo-Guerrero and Vallejo (2005a,b), Vallejo et al. (2006), and Bolton et al. (2008). In these investigations a number of interesting experimental and micromechanical [discrete-element method (DEM)] studies have considered the influence of particle crushing on the material response. Time effects were not studied in these investigations.

The hypothetical mechanistic picture of time effects in granular materials is based on an assembly of soil grains, as shown in Fig. 3(a). It shows an assembly of grains that has been loaded up to a given stress difference and either creep (time-dependent strains of material under constant stresses) or stress relaxation (time-dependent reduction in stresses in material under constant strain, i.e., zero change in strain) occurs from this point. The diagram shows the force chains (Cundall et al. 1982) down through the assembly. The grain in the middle fractures just before the initiation of either of these two types of time effects. The responses of the grain assembly are quite different for the two phenomena. Fig. 3(b) shows what happens during creep in which the vertical stress is held constant. The assembly adjusts its structure to carry the vertical stress. This requires adjustment of the

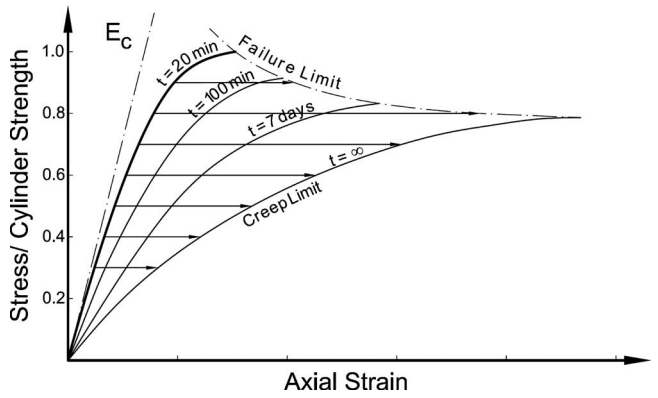

Fig. 4. Effect of time on strength of concrete specimens (after Rűsch 1960)

grains and it results in some vertical deformation and new force chains are created to match the externally applied stress. The redundancy in the grain structure allows new force chains to be created and engage other grains that may break. However, slowly the amount of breakage will reduce and the creep will slow down with time, just as observed in the experiments.

Fig. 3(c) shows what happens in the stress relaxation experiment. After the grain has broken, the grain structure is not able to carry the vertical stress, but since the assembly is prevented from vertical deformation, the stress relaxes. New force chains are created around the broken grain, which does not carry any load. It is the small amounts of grain movement in the creep tests that allow new contacts to be created and forces to be carried through the grain skeleton. Without this adjustment and consequent deformation to achieve the adjustment, the grain structure is able to transmit only a reduced load and stress relaxation is the consequence. It can also be seen that if a lower limit to the relaxed stress exists, then it depends on the grain strength rather than its frictional properties.

As seen in Fig. 1, the experiments on Antelope Valley sand showed considerable differences in their stress-strain relations after one day of creep and one day of relaxation. Similar results were obtained for crushed coral sand, as seen in Fig. 2. These differences were not the same for the two sands, but they may be explained in terms of different grain strengths.

It also follows from this picture that the volumetric strain observed with time will be contractive, as also observed by Coop et al. (2004), because upon crushing the proportion of smaller particles tends to increase, and these can be accommodated within the void space between the larger particles, resulting in an overall contraction of the material. The signature volumetric strain of time effects in granular materials is therefore always contractive even if this might be superimposed on a dilative shearing response. Such contraction was observed for both Antelope Valley sand and for crushed coral sand.

With only friction (and slippage when the frictional resistance is overcome) and particle breakage (when the strengths of the particles are overcome) as basic behavior constituents, how can the observed time effects be explained for granular materials? Experiments on rock and concrete specimens have clearly shown that their strengths are strongly dependent on time (Rűsch 1960; Cristescu and Hunsche 1998). This phenomenon is referred to as static fatigue or delayed fracture (Lemaitre and Chaboche 1990; Callister 2005). Fig. 4 shows the stress-strain-time behavior obtained from tests on concrete cylinders (Rűsch 1960). As the load on the cylinders are held constant below the short-term fracture load, the time to fracture increases with decreasing load until fracture does not occur at all at around 80% of the short-term fracture load. Single sand particles behave similarly in the sense that their crushing strengths are time dependent. Static fatigue appears to be at the root of time effects in granular materials, and a more detailed review and explanation of this phenomenon is given by Lade and Karimpour (2010).

Presented here is a study of time effects in Virginia Beach sand. A series of drained triaxial compression tests was initially performed at confining pressures from 250 to 14,000 kPa to determine where significant particle crushing would occur. Subsequently, it was decided to study time effects for this sand at a constant effective confining pressure of 8,000 kPa. Thus, the states of stress during shearing of the triaxial specimens correspond to those experienced near tips of relatively long piles (15–30 m or 50–100 ft), near the bottom of deep wells, and near deep tunnels.

Sand Tested

Virginia Beach sand was used in the entire experimental program. The portion contained between the No. 20 and No. 40 U.S. (0.850–0.425 mm), i.e., a rather uniform gradation, was used in the tests, such that crushing would be enhanced due to testing, and this would result in identifiable changes in the gradation curve. Virginia Beach sand is composed of subangular to subrounded grains consisting mainly of quartz and some feldspar. The characteristics of the portion of sand tested are summarized as follows: mean diameter, 0.638 mm; coefficient of uniformity, 1.40; specific gravity, 2.65; maximum void ratio, 0.759; and minimum void ratio, 0.532.

Equipment, Specimen Preparation, and Testing Procedures

All the compression tests on beach sand were performed in a triaxial cell with a confining pressure capacity of 14,000 kPa. Triaxial specimens with average diameter=36.6 mm and average height=107.7 mm were created by dry pluviation with approximately 50-cm drop height. The initial void ratio was 0.537 $\pm$0.004 corresponding to a relative density of 98%. The specimens were initially enclosed in a 0.65-mm-thick latex rubber membrane and filter stones were used in both ends. Even though the filter stones provided full friction at the ends, the specimens were observed to deform essentially as right cylinders due to the high confining pressures employed in this study.

To avoid membrane puncture during testing, the latex rubber membrane containing the specimen was smeared with a layer of silicone grease (dow corning high vacuum), and three layers of 0.28-mm continuous rubber sheets with layers of silicone grease were wrapped around the specimen. A vertical strip of glue (Barge) was smeared at the edge of each complete wrap to glue the layers together. In addition, on the last vertical wrap edge, a strip of liquid latex rubber was applied and allowed to dry. This four-layer-thick assembly of membranes was sealed by two O rings at each end.

The cell pressure was supplied from a nitrogen bottle and controlled by a high pressure regulator. To avoid nitrogen dissolving in the initially deaired cell water from reaching the specimen within the time of the test (by dissolution into the cell water at a

pressure of 8,200 kPa, traveling through the cell water by diffusion, penetrating through the membranes, and coming out of solution inside the specimen where the back pressure is a nominal 200 kPa) and produce a false volume change response, the nitrogen pressure was applied at the end of a long spiral of stainless steel tubing full of deaired water. Since gas travels by diffusion, a sufficiently long tube would prevent the nitrogen from reaching the specimen within the time of the test.

The initially dry specimen was saturated using the CO_2 method (Lade and Duncan 1973) and Skempton's B value $(=\Delta u/\Delta\sigma_3)$ (Skempton 1954) was determined to ensure that the specimen was fully saturated. Based on the dense state of the specimens, B values of 0.94 indicated acceptable degrees of saturation for the drained tests in this study.

Following saturation of the specimen, the isotropic confining pressure was increased in steps of 500 kPa until the desired effective confining pressure of 8,000 kPa was reached. For each increment in confining pressure, the specimen was allowed to creep for 2 min before the volume change and the axial deformation were recorded. The confining pressure was then increased to the next value. After the effective confining pressure of 8,000 kPa had been achieved, the specimen was allowed to creep for 45 min before shearing was initiated.

Unlike consolidation, there is no distinct time period after which creep has terminated. Rather, creep progresses with logarithmic time, and no particular time is ideal for application of the next pressure increment. The short periods of time allowed at each new confining pressure were not sufficient to reach any particular amount or proportion of creep, but it was judged to be the most practical method of reaching the high confining pressure of 8,000 kPa under controllable circumstances while taking readings along the way. Waiting for longer time periods would produce a stress-strain relation that would be similar to that produced after 2 min of creep. The 45 min of creep at 8,000 kPa allowed the creep rate to reduce to a small value and allowed the operator to check all test settings and data logging devices before initiating application of the deviator stress. Because creep progresses with log(time), there does not appear to be any scientific way of choosing any particular time for creep before continuation to the next load step.

The deviator load was applied to the specimen under deformation control or under load control with the possibility of switching between the two types of control. The deformation control was supplied by a triscan 100 advanced digital triaxial system whose frame had a capacity of 50 kN. The load control device consisted of a Bellofram (rolling diaphragm) cylinder operated by regulated air pressure from the same house pressure line as employed for the back pressure. The axial deviator load was measured by a 45-kN load cell, and the axial deformation was measured by a digital dial gauge attached to the piston.

During a creep test the cross-sectional area of the specimen was determined from the measured volume change (expelled water) and axial deformation, and the deviator stress was maintained constant by frequently calculating the cross-sectional area and increasing the air pressure in the Bellofram cylinder to increase the deviator load to achieve the desired constant deviator stress.

During an experiment the axial deviator load, the axial deformation, the volume change, and the time were recorded. Referring to the study by Lade and Liu (1998), careful determination of strains from this classical system are as accurate as those measured by a much more sophisticated and elaborate measurement systems that measure movement of points directly on the specimen.

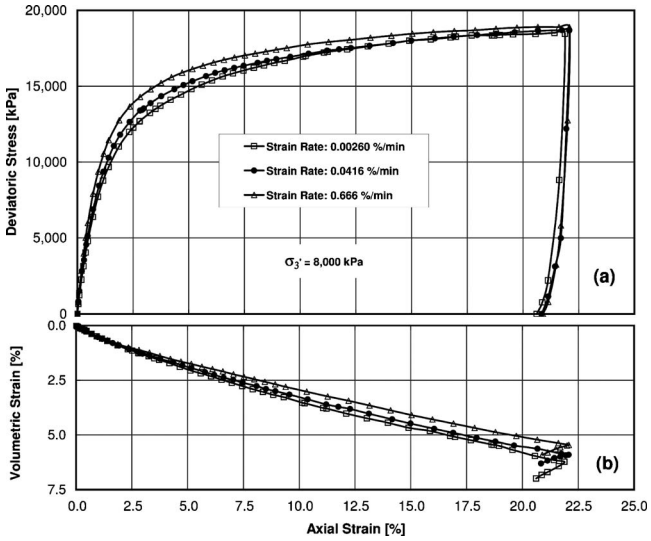

Fig. 5. Effect of strain rate on (a) stress-strain; (b) volume change relations for Virginia Beach sand

Experimental Program

While the initial void ratio and the effective confining pressure were kept constant at 8,000 kPa in this study, a systematic experimental program was performed to explore (1) effects of loading strain rate on the stress-strain, strength, and volume change behavior; (2) effects of loading strain rate on subsequent amount of creep; (3) effects of loading strain rate on subsequent amount of stress relaxation; (4) effects of small axial strains on amount of stress relaxation; and (5) the relation between time effects, energy input, and particle crushing.

Experimental Results

Effects of Loading Strain Rate on Stress-Strain Behavior

It has been found that effects of strain rate on stress-strain, strength, and volume change relations obtained from triaxial compression tests are small to negligible for sands. This was explained in a comprehensive review by Augustesen et al. (2004), and it was concluded from experimental studies by Yamamuro and Lade (1993), Matsushita et al. (1999), Santucci de Magistris and Tatsuoka (1999), Tatsuoka et al. (2000, 2002, 2006), Di Benedetto et al. (2002), Kuwano and Jardine (2002), AnhDan et al. (2006), Kiyota and Tatsuoka (2006), Lade (2007), and Lade et al. (2009, 2010).

Three triaxial compression tests were performed on dense Virginia Beach sand with the deformation rates of 0.0028, 0.0448, and 0.7168 mm/min. These correspond to strain rates of 0.002 60, 0.0416, and 0.666%/min; i.e., the maximum strain rate is 256 times higher than the minimum strain rate. Thus, to reach similar axial strains of 22%, where failure occurred, the experiments lasted for approximately 6 days, 9 h, and 33 min, respectively.

The stress-strain and volume change curves from the tests are

shown in Fig. 5. It is seen that specimens sheared at higher strain rates produce slightly stiffer response and slightly higher deviator stresses in the middle range of the axial strain. However, when the axial strain approaches the vicinity of failure, the curves converge and almost the same magnitude of deviator stress is observed for all three tests. For these tests, friction angles calculated at their peak deviator stresses increased with strain rate and achieved values of 27.7°, 27.8°, and 27.9°.

Fig. 5(b) shows that the experiment with the lowest strain rate exhibits more volumetric contraction. In these tests the volumetric strains to failure of 6.23, 5.77, and 5.33% were observed for the slowest to the fastest test.

It is clear from these experiments that there is some effect of strain rate on the stress-strain and volume change behavior, while the effects on failure are very small but still consistent with the magnitudes of the strain rates. This is due to the time-dependent fracture, i.e., the static fatigue of the sand particles. There is more time for the particles to crush in the slower tests and more contractive volume changes are therefore observed in these tests. To show the consistency in the study, the stress-strain and volume change relations presented in Fig. 5 will be used as reference curves for the following investigations.

Effects of Loading Strain Rate on Subsequent Creep

Previous experiments to study creep and relaxation were all performed with the same loading strain rate. Thus, the effects of the initial loading strain rate on the subsequent amounts of creep and stress relaxation were not investigated before. Therefore, three specimens were sheared with strain rates of 0.002 60, 0.0416, and 0.666%/min up to points on the stress-strain curves where $[(\sigma_1-\sigma_3),\varepsilon_1]=[12,850\ \text{kPa},\ 3.05\%]$, [13,510 kPa, 3.00%], and [14,150 kPa, 2.91%], i.e., at approximately 70% of their deviator strengths.

The total energy input per unit volume of specimen during each experiment was calculated for each test according to the expression

$$E=\sum \sigma_c'\cdot\Delta\varepsilon_v+\sum(\sigma_1-\sigma_3)\cdot\Delta\varepsilon_a \tag{1}$$

in which σ_c'=effective confining pressure; $\Delta\varepsilon_v$=increment in volumetric strain; $(\sigma_1-\sigma_3)$=deviator stress; and $\Delta\varepsilon_a$=increment in axial strain. The points on the stress-strain curves at approximately 70% of the deviator strengths correspond to points where the energy input per unit volume calculated from Eq. (1) has reached the same level of 581 kN m/m^3=581 kN/m^2=581 kPa. At these points, the load was held constant by switching from deformation control to load control and creep observations were initiated and continued for one day (1,440 min).

The reason for initiation of the creep stages at the same amount of energy input is that it has been found that particle crushing is related to the energy input (Lade et al. 1996). However, the occurrence of static fatigue prevents the specimens loaded at different strain rates from being at the same condition in terms of the amount of particle crushing and the grain structure. Thus, to begin observations of creep at the same amount of energy input is one option when studying the subsequent creep or stress relaxation. These tests could also have been initiated at a common deviator stress or a common axial strain.

Fig. 6 shows stress-strain and volume change curves for the three tests together with superimposed reference curves from Fig. 5. Within the scatter in such experiments, the portions of the stress-strain and volume change curves obtained during constant strain rate shearing coincide with the reference curves, thus indicating the repeatability of the tests.

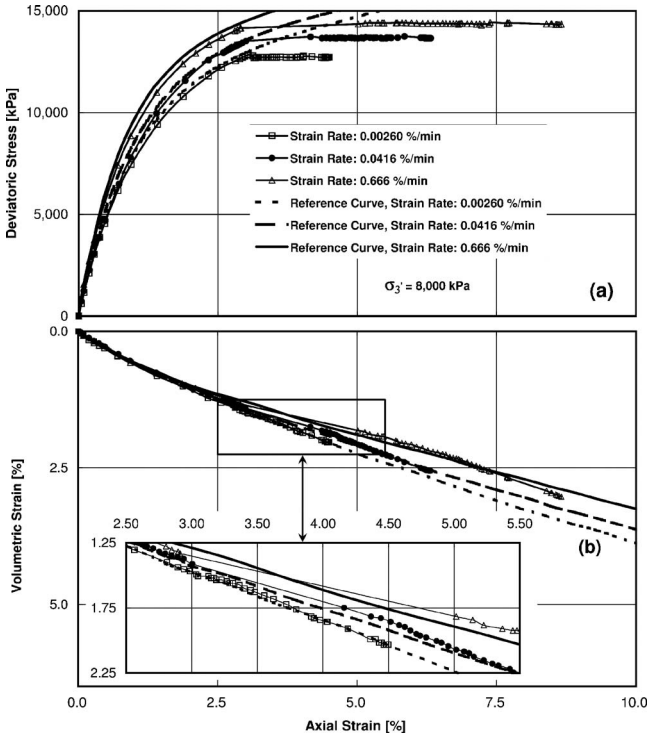

Fig. 6. Effects of initial loading strain rate in (a) amount of creep; (b) volume change behavior. The change from strain control to stress control with creep occurs near 3% axial strain. The volumetric strain developments are magnified in the lower diagram in the range of axial strains from 2.5 to 5.5%.

It is clearly seen that experiments performed with the higher strain rates show more creep within one day. Moreover, Fig. 6(a) shows that there is a jump in the axial strain as soon as the loading is switched from deformation control to load control to maintain constant deviator stress. This jump is significantly more pronounced in tests sheared with higher strain rates. Furthermore, the volume change curves, shown in Fig. 6(b), indicate that when the switch occurs, the volumetric strains jump along the reference curves. In fact, no tendency to change the volume change curve away from the reference curve appears in these experiments.

The same behavior was observed for tests performed on Antelope Valley sand presented by Lade (2007), and this indicates that the same potential function may be used for modeling the inelastic creep strains. However, this is different from the experiments on crushed coral sand reported by Lade et al. (2010), which showed more contraction than indicated by the corresponding reference curves.

Fig. 7 shows the axial and volumetric creep strains plotted versus log(time). Following the first 5–10 min the axial creep strains progress in time at similar rates, i.e., the curves on Fig. 7(a) tend to become parallel, although slightly increasing creep strain rates seem to occur later with increasing initial strain rate. The volumetric creep strains, shown in Fig. 7(b), exhibit a similar pattern. However, the initial adjustments occur at faster rates for the tests initially sheared at the higher strain rates.

The total axial creep strains observed after one day of creep, shown in Fig. 7(a) as the differences between the strains at 1,440 min and at 0.01 min, were 5.61, 3.31, and 1.45% for the tests with

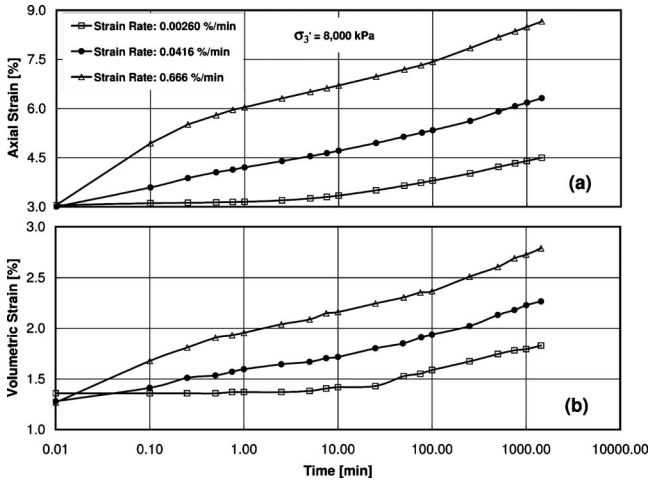

Fig. 7. Variation in (a) axial strain; (b) volumetric strain with log(time) during creep following shearing with different strain rates

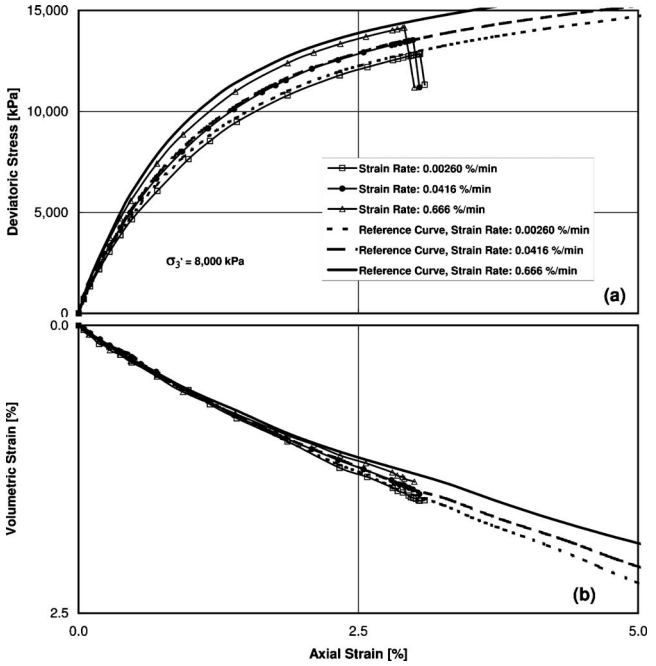

Fig. 8. Effects of initial loading strain rate on (a) amount of stress relaxation; (b) volume change behavior

the highest to the lowest initial strain rate, respectively. The corresponding volumetric strains were 1.49, 0.96, and 0.46%. The reason that larger amounts of creep axial and volumetric strains occur in the tests with higher initial loading rates is, in part, that very little time was available for the time-dependent crushing to occur during initial loading, while much more time was available for crushing at higher average shear stresses in these tests.

Fig. 7 indicates that almost no creep occurs within the first 8 min for the specimen sheared with lowest strain rate of 0.0026%/min. For this slow loading rate the specimen has had sufficient time that particles have crushed and the grain structure has been modified to resist the imposed load. Thus, stable force chains have been formed and there is consequently no immediate reaction to the switch from deformation to load control. However, for the specimen loaded at the middle strain rate of 0.0416%/min, the axial and volumetric creep strains vary almost linearly with log(time).

For the specimen initially loaded at the highest rate of 0.666%/min, the highest creep rate occurs in the first 40 s. Although there is only little difference in the amount of crushing between the three specimens, as discussed below, the grain structure in the specimen with the highest rate must be different and not sufficiently stable to carry the load over longer periods of time. This is because the grains have not had sufficient time to crush and adjust to their optimum positions for creation of stable force chains to carry the sustained load. When the switch from deformation control to load control occurred, a number of grains, which previously did not have sufficient time to crush according to the static fatigue relation indicated in Fig. 4, now have the time required to crush under the sustained load. This causes the grain structure to adjust as necessary to hold the imposed load. It was observed during the switch from deformation to load control that the immediate response was a drop in the load carrying capability of the specimen, i.e., a response similar to the stress relaxation. This was quickly followed by a readjustment of the grain structure and reestablishments of force chains to resist the imposed load.

Effects of Loading Strain Rate on Subsequent Stress Relaxation

As in the creep experiments, tests were performed to study stress relaxation after initial loading under strain control. Three tests were performed on dense Virginia Beach sand with loading under initial strain rates of 0.002 60, 0.0416, and 0.666%/min up to points on the stress-strain curves where $[(\sigma_1-\sigma_3),\varepsilon_1]$ $=[12{,}850\ \text{kPa}, 3.05\%]$, $[13{,}530\ \text{kPa}, 2.99\%]$, and $[14{,}150\ \text{kPa}, 2.91\%]$ corresponding to approximately 70% of their deviator strengths, respectively. Thus, similar amounts of initial energy/volume (592 kPa) were applied for the stress relaxation experiments as for the creep experiments. At these points, the deformation was stopped and the stress was allowed to relax for one day (1,440 min).

The stress-strain and volume change relations obtained from these tests are shown in Fig. 8. The almost vertical lines initiating from the highest points on each stress-strain curve show relaxation, which corresponds to reduction in the deviator stresses. It is again observed that there is good correspondence between the initial portions of the tests with stress relaxation and the reference curves from Fig. 5. Fig. 8(b) indicates that the three specimens exhibit extremely little volumetric strain during the stress relaxation phases of the tests. Similar results were obtained for the experiments on Antelope Valley sand while the tests on crushed coral sand exhibited some volumetric contraction during stress relaxation. The drained stress relaxation experiments on Virginia Beach sand show essentially zero volumetric strains. Undrained stress relaxation tests, in which no strains would occur at all, would therefore result in negligible pore pressure built-up.

Corresponding to the initial strain rates of 0.002 60, 0.0416, and 0.666%/min, the total stress relaxation observed in the three experiments amounted to 1,530, 2,340, and 2,970 kPa, respectively. Thus, the test with the highest initial loading strain rate exhibits the largest amount of stress relaxation. Fig. 9 shows the stress relaxation plotted versus log(time), both in terms of the drop in deviator stress and in terms of the actual deviator stress. The specimen loaded at the slowest rate does not begin stress relaxation until after about 2–5 min, whereas the test with the fastest loading rate shows immediate high rate of stress relaxation. Although relaxation commences at points corresponding

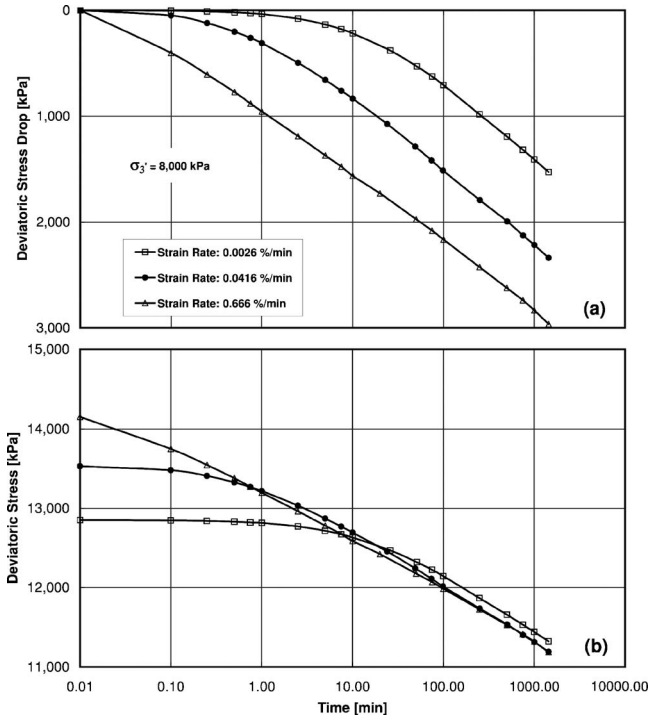

Fig. 9. Variation in (a) deviator stress drop; (b) actual deviator stress with log(time) during stress relaxation following shearing with different strain rates

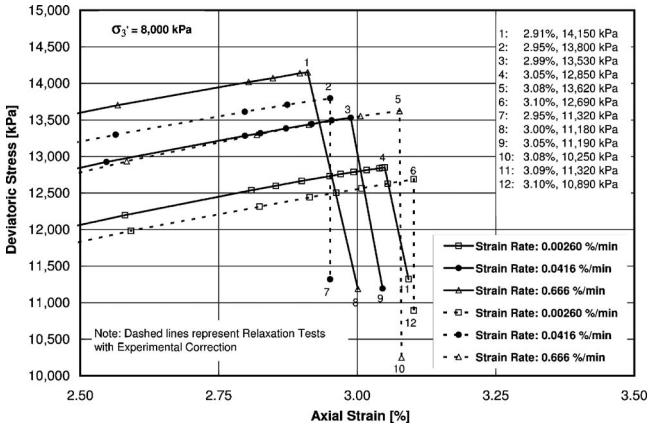

Fig. 10. Effects of small axial strains on stress relaxation in triaxial compression tests. The coordinates of the 12 points are given in the inserted table.

to the same energy input, these points correspond to three different values of deviator stress, as shown in Fig. 9(b), but all three curves converge to the same line, and after a little less than 100 min the stress relaxation progresses at the same rate and the deviator stresses achieve the same magnitudes in the three specimens.

The observed stress relaxation behavior may also be related to the mechanistic picture presented above and illustrated in Fig. 3. During the initial loading under deformation control there was somewhat less crushing occurring in the high than in the low strain rate tests, as discussed below. When the axial deformation was stopped in the high strain rate test, a number of grains, which previously did not have sufficient time to crush according to the static fatigue relation indicated in Fig. 4, now immediately begin to crush. This causes the grain structure to adjust, but since no deformation occurs, the stress relaxes. In comparison, the grains in the specimen initially sheared at the slow strain rate had sufficient time to crush as required to be in essential equilibrium with its static fatigue behavior and therefore did not show so much stress relaxation at the beginning of this phase.

Effects of Small Axial Strains on Stress Relaxation

There is a fundamental experimental difficulty in performing stress relaxation tests. While the axial displacement of the loading machine is completely stopped (and the triaxial setup is stiff to avoid significant compression of interfaces, etc.), it is necessary to measure the drop in axial load on the specimen. This requires a load cell in series with the triaxial specimen inside the load frame that holds the deformation across the setup at zero. To register a decrease in load due to stress relaxation, the load cell must expand, and this expansion is countered by the specimen; i.e., the specimen is compressed in the axial direction. The load applied to the specimen and measured on the load cell is consequently too high to correspond to true stress relaxation at zero axial strain.

To investigate the sensitivity of the measured stress relaxation to the small amounts of axial deformation imposed by expansion of the load cell during decreasing load, three experiments were performed in which the specimens were initially loaded at the same three deformation rates used in the experiments presented above. As in the previous tests, the axial deformation of the specimen in these sensitivity check tests was continuously monitored by a digital dial gauge. The dial gauge reading was very accurately maintained constant by small adjustments in the displacement of the deformation control loading machine. The results of these three experiments are compared in Fig. 10 with the results of the stress relaxation experiments presented above. In this magnified diagram, the slightly inclined lines indicate stress relaxation without correction, while the vertical lines include experimental correction so the results correspond to true stress relaxation at zero strain. Comparing individual pairs of tests from those initially loaded at the lowest to the highest strain rates, the differences in amount of stress relaxation in one day are $(1{,}800-1{,}530)=270$ kPa, $(2{,}470-2{,}340)=130$ kPa, and $(3{,}370-2{,}970)=400$ kPa. These errors show that the true stress relaxation values are underestimated by 5–15%. The stiffness of the load cell employed in these experiments relates to the slopes of the slightly inclined relaxation curves and it is approximately 36×10^3 kN/m. It is possible that an even stiffer load cell would have reduced the errors in the amounts of stress relaxation measured, thus avoiding the continuous adjustment in displacement of the deformation control loading machine.

Relations between Time Effects and Particle Crushing

When the stresses on soil particles exceed their strengths, particle breakage occurs. This particle strength is dependent on time as discussed and indicated in Fig. 4, and this is the fundamental behavior that accounts for time effects in granular materials. Very little crushing occurs at low confining pressures, while experiments show that considerable crushing occurs at higher confining pressures where the time effects are also pronounced. The amount of crushing relates to the amount of energy input to the soil. Thus, time effects are related to energy input and crushing.

To determine the amount of crushing that occurred for each

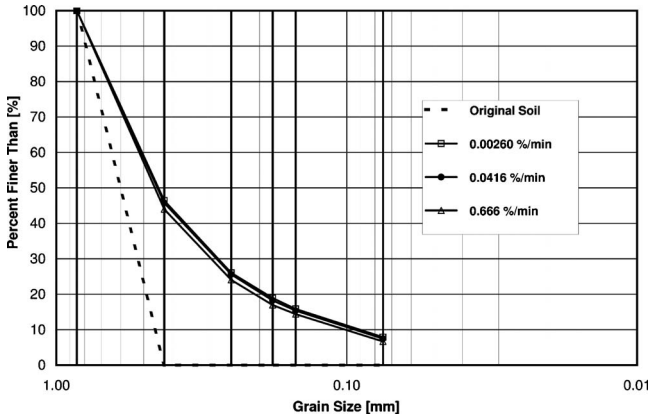

Fig. 11. Grain size distribution curves following tests performed with different initial loading strain rates to failure at 22% axial strain, shown in Fig. 5

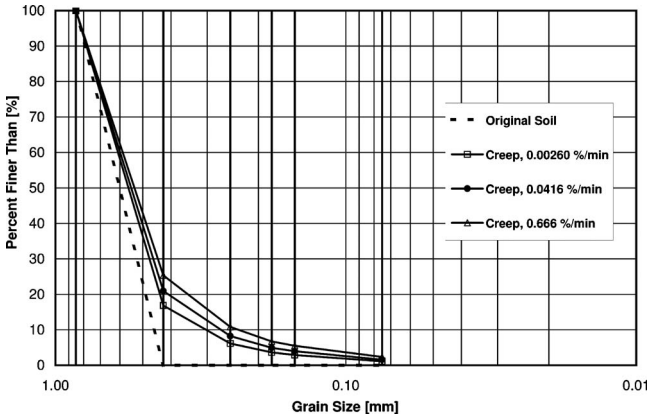

Fig. 12. Grain size distribution curves determined for tests performed with different initial loading strain rates to stress level of approximately 70% followed by creep for 1440 min, shown in Fig. 6

test section, separate isotropic compression tests and triaxial compression tests were performed with shearing up to and stopped at the stress points at which either creep or stress relaxation was initiated in the experiments discussed above. Thus, it was possible to dissect and analyze each experiment in terms of energy input for each section and relate it to the corresponding amount of crushing determined from the sieve analyses. The sieve analysis on the crushed sand (197 g) from each small specimen was performed using small sieves with diameter of 10 cm (4 in.) and sieving one-third of each specimen at a time to obtain accurate results.

Fig. 11 illustrates the grain size distribution curves for the specimens that were sheared to demonstrate the effect of strain rate on stress-strain behavior shown in Fig. 5. The change in grain size distribution due to isotropic compression up to 8,000 kPa is essentially indistinguishable from the initial grain size distribution curve for the original soil indicated by the dashed lines. This will be further discussed in connection with Fig. 15. Because the energy input depends on the axial strain, the tests were all terminated after failure at the same axial strain of about 22%. However, the experiments showed slightly different energy inputs per unit volume with the highest strain rate corresponding to the lowest energy input/volume as follows: 4,230, 4,250, and 3,980 kPa. While the grain size curves in Fig. 11 show almost the same amounts of crushing, the small differences indicated by the relative locations of the curves reflect the differences in energy input. However, the differences are within the scatter in the sieve analyses.

Fig. 12 shows the grain size curves for the experiments with creep following the initial shearing at three different strain rates, whose results were shown in Fig. 6. The specimens were sheared up to about 3% axial strain at three different initial strain rates, which had significant impact on the subsequent creep behavior. After 1,440 min of creep it was observed that the higher the initial strain rate, the more axial creep strain is produced. Therefore, more energy has been applied to the specimens sheared at higher strain rate, and it is expected that specimens in tests with higher initial rate of straining experience more crushing. This relation is confirmed as seen in Fig. 12 in which the grain size curve of experiments with higher loading strain rate has moved furthest out relative to the original soil grain size curve.

For the tests with stress relaxation shown in Fig. 8, the specimens were also sheared up to about 3% axial strain at three different initial strain rates. These specimens had similar energy input per unit volume (598, 590, and 588 kPa from fastest to slowest), and similar amounts of stress relaxation, irrespective of their initial loading strain rates. The energy input during stress relaxation of Virginia Beach sand is essentially zero since there are negligible axial and volumetric strains occurring during this stage of the tests. Thus, the energy input/volume and crushing observed in these tests essentially correspond to those at the points of initiation of stress relaxation. Consequently, the amounts of crushing are expected to be similar in the three tests, as also confirmed from the grain size curves in Fig. 13. In fact, it may be concluded that the amount of stress relaxation is not discernable on the basis of the amount of crushing because negligible energy input and negligible crushing occurs during stress relaxation. The crushing due to creep in the tests shown in Fig. 6 can therefore be determined by subtracting the grain size curves in Fig. 13 from the curves in Fig. 12. As expected, there is more crushing occurring in the test with the largest amount of creep.

To quantify the grain crushing occurring in each test it is necessary to represent this phenomenon by a single number such as a particle breakage factor. Different particle breakage factors have been suggested in literature by, e.g., Marsal (1967), Lee and Farhoomand (1967), Hardin (1985), and Lade et al. (1996). These

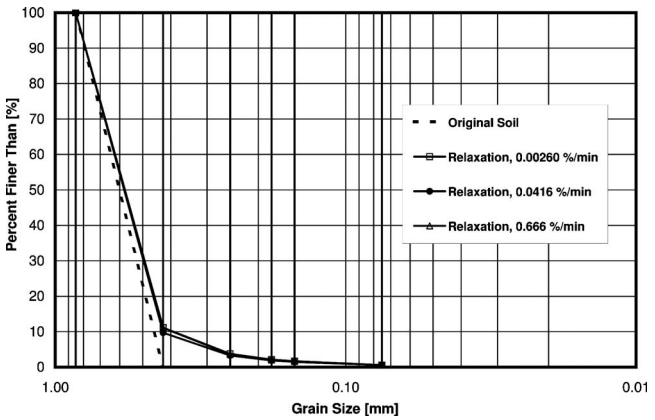

Fig. 13. Grain size distribution curves determined for tests performed with different initial loading strain rates to stress level of approximately 70% followed by stress relaxation for 1,440 min, shown in Fig. 8

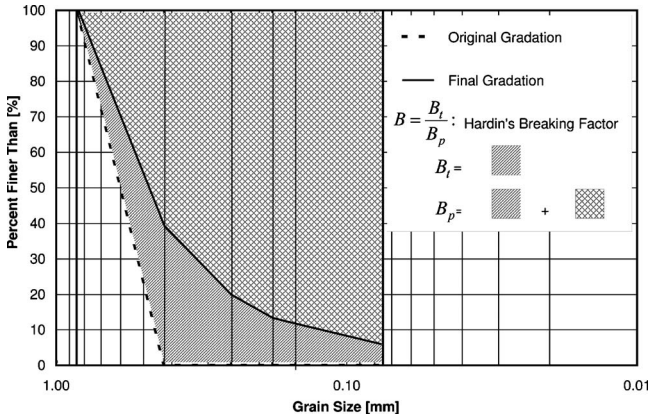

Fig. 14. Definition of particle breakage factor proposed by Hardin (1985)

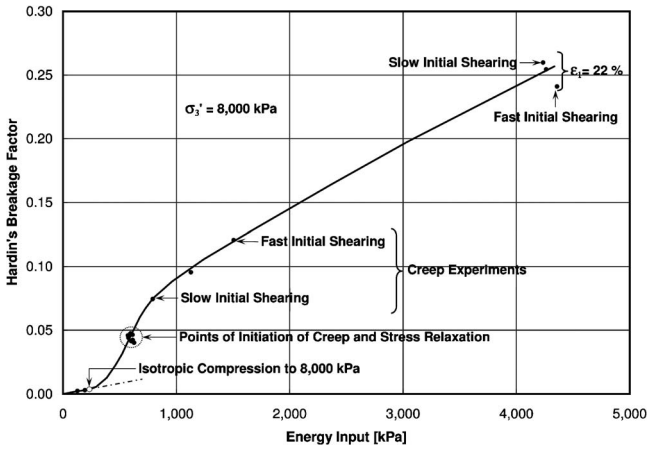

Fig. 15. Relation between Hardin's particle breakage factor and input energy to all triaxial compression tests performed on Virginia Beach sand with confining pressure of 8,000 kPa. The experiments that end with axial strains of 22% are shown in Fig. 5 and the creep experiments are shown in Fig. 6.

breakage factors are based on either single particle size as the key measurement or on aggregate changes in overall grain size distribution. Hardin's particle breakage factor appears to be most appropriate for the present investigation, and it is defined as

$$B = \frac{B_p}{B_t} \tag{2}$$

in which B_t=total breakage represented by the area between the original gradation curve and final gradation curve, as indicated in Fig. 14, and B_p=breakage potential represented by the area over the original grain size distribution curve and limited to U.S. sieve No. 200. This factor has the lower limit of zero corresponding to no crushing, and a theoretical upper limit of unity showing 100% crushing such that all crushed particles would pass through the No. 200 sieve.

Relations between Time Effects, Energy Input, and Particle Crushing

The energy input per unit volume was calculated from Eq. (1) for each section consisting of (1) isotropic compression; (2) shearing at constant strain rate; and (3) creep or stress relaxation. In addition, Hardin's particle breakage factor has been determined for each experiment performed for this study and plotted versus the corresponding energy input/volume in Fig. 15. The results form a pattern for the all tests performed with a confining pressure of 8,000 kPa. At the high end are the three experiments performed to failure and stopped at an axial strain of 22%. The small differences in energy input/volume in the experiments with different loading strain rates are not quite matched by similar differences in amount of crushing. However, these differences are small and may be due to scatter.

The cluster of experimental points near the origin corresponds to experiments with energy input/volume and crushing up to the points of initiation of creep and stress relaxation. The experimental points all come from the stress relaxation tests in which no further energy input/volume or crushing occurs after these points. It is seen that very little crushing occurs due to isotropic compression up to 8,000 kPa, represented in Fig. 15 by the dotted curve from the origin. Similarly, there is very little crushing at the beginning of shearing, where the shear stresses and the shear strains are still relatively small.

The three points above the points of initiation of creep and stress relaxation correspond to the creep experiments shown in Fig. 6. Once the creep strains progress at constant and relatively high shear stresses, considerable amounts of crushing occur nearly in proportion to the energy input/volume.

The results presented in Figs. 11–13 demonstrate the close relations between time effects, energy input/volume, and particle crushing. The energy input includes effects of frictional sliding and rearrangement of particles, which dominates the behavior at lower confining pressures where very little crushing and negligible time effects are observed in granular materials with strong particles. This is indicated by the initially modest slope of the crushing curve in Fig. 15. However, as the confining pressure, the shear stresses, and the shear strains increase, the particle crushing begins to dominate the behavior. At these higher stresses, the particles are held tightly together, and it is the particle crushing that produces strains rather than rearrangement and frictional sliding between intact grains. Thus, energy input is predominantly expended on particle crushing at higher stresses. Since particle crushing is a time-dependent phenomenon described as static fatigue or delayed fracture, as reviewed above, the close relation between time effects and crushing in granular materials has been established.

Conclusion

Time effects are associated with particle crushing and can occur in granular materials under any condition in which particle crushing is possible. This important effect can occur at low pressures for weaker granular materials, or at high pressures encountered in geotechnical applications such as pile driving and blasting, near the bottom of deep wells, and near deep tunnels.

An investigation of the relation between time effects in granular materials and time-dependent particle crushing, known as static fatigue, has been performed on Virginia Beach sand, consisting mainly of strong particles of quartz and some feldspar. It included studies of (1) effects of loading strain rate on the stress-strain, strength, and volume change behaviors; (2) effects of loading strain rate on subsequent amount of creep; (3) effects of loading strain rate on subsequent amount of stress relaxation; (4) effects of small axial strains on amount of stress relaxation; and

(5) the relation between time effects, energy input/volume, and particle crushing.

The results of this investigation demonstrate the close relations between time effects, energy input/volume, and particle crushing, as characterized by Hardin's particle breakage factor. The stress-strain response of granular materials can be considered as a combination of frictional sliding and particle crushing. Frictional sliding is the most important component of deformation at lower stresses, while it plays a much smaller role in the behavior of granular materials at high stresses where particle crushing dominates the deformations. The energy input includes effects of frictional sliding and rearrangement of particles, which dominates the behavior at lower confining pressures where very little crushing and negligible time effects are observed in granular materials with strong particles. As the confining pressure, the shear stresses, and the shear strains increase, the particle crushing begins to dominate the behavior. At these higher stresses, the particles are held tightly together, and it is the particle crushing that produces strains rather than rearrangement and frictional sliding between intact grains. Thus, energy input is predominantly expended on particle crushing at higher stresses. Since particle crushing is a time-dependent phenomenon described as static fatigue or delayed fracture, as reviewed above, the close relation between time effects and crushing in granular materials has been established.

Only small effects of loading strain rate on stress-strain, volume change, and strength behavior were observed. However, a higher initial loading strain rate up to a stress level of approximately 70% resulted in subsequent higher creep axial strain, higher energy input/volume, and higher amounts of grain crushing. The creep volume change relation followed that obtained during continued static loading at the same rate.

The initial loading rate did not appear to have much influence on the subsequent stress relaxation. Since negligible additional energy input/volume was observed during stress relaxation, the amount of additional crushing was negligible, and the amount of stress relaxation could not be related to the amount of crushing. It was also observed that small amounts of axial strains occurring during stress relaxation, caused by expansion of the load cell, resulted in slightly smaller amounts of stress relaxation than measured in tests where zero axial strain was maintained.

References

AnhDan, L., Tatsuoka, F., and Koseki, J. (2006). "Viscous effects on the stress-strain behavior of gravelly soil in drained triaxial compression." *Geotech. Test. J.*, 29(4), 330–340.

Augustesen, A., Liingaard, M., and Lade, P. V. (2004). "Evaluation of time dependent behavior of soils." *Int. J. Geomech.*, 4(3), 137–156.

Bolton, M. D., Nakata, Y., and Cheng, Y. P. (2008). "Micro- and macro-mechanical behaviour of DEM crushable materials." *Geotechnique*, 58(6), 471–480.

Callister, W. D., Jr. (2005). *Materials science and engineering*, Wiley, New York.

Cheng, Y. P., Nakata, Y., and Bolton, M. D. (2003). "Discrete element simulation of crushable soil." *Geotechnique*, 53(7), 633–641.

Coop, M. R., Sorensen, K. K., Bodas Freitas, T., and Georgoutsos, G. (2004). "Particle breakage during shearing of carbonate sand." *Geotechnique*, 54(3), 157–163.

Cristescu, N. D., and Hunsche, U. (1998). *Time effects in rock mechanics*, Wiley, New York.

Cundall, P. A., Drescher, A., and Strack, O. D. L. (1982). "Numerical experiments on granular assemblies: Measurements and observations." *IUTAM Conf. Deformation and Failure of Granular Materials*, P. A. Vermeer and H. J. Luger, eds., Balkema, Rotterdam, The Netherlands, 355–370.

Di Benedetto, H., Tatsuoka, F., and Ishihara, M. (2002). "Time-dependent shear deformation characteristics of sand and their constitutive modeling." *Soils Found.*, 42(2), 1–22.

Hardin, B. O. (1985). "Crushing of soil particles." *J. Geotech. Engrg.*, 111(10), 1177–1192.

Kiyota, T., and Tatsuoka, F. (2006). "Viscous property of loose sand in triaxial compression, extension and cyclic loading." *Soils Found.*, 46(5), 665–684.

Kou, S. Q., Liu, H. Y., Lindqvist, P.-A., Tang, C. A., and Xu, X. H. (2001). "Numerical investigation of particle breakage as applied to mechanical crushing. Part II: Interparticle breakage." *Int. J. Rock Mech. Min. Sci.*, 38, 1163–1172.

Kuwano, R., and Jardine, R. (2002). "On measuring creep behaviour in granular materials through triaxial testing." *Can. Geotech. J.*, 39(5), 1061–1074.

Lade, P. V. (2007). "Experimental study and analysis of creep and stress relaxation in granular materials." *Proc., Geo-Denver* (CD-ROM), Denver.

Lade, P. V., and Duncan, J. M. (1973). "Cubical triaxial tests on cohesionless soil." *J. Soil Mech. and Found. Div.*, 99(*SM10*), 793–812.

Lade, P. V., and Karimpour, H. (2010). "Static fatigue controls particle crushing and time effects in granular materials." *Soils Found.*, in press.

Lade, P. V., Liggio, C. D., Jr., and Nam, J. (2009). "Strain rate, creep and stress drop-creep experiments on crushed coral sand." *J. Geotech. Geoenviron. Eng.*, 135(7), 941–953.

Lade, P. V., and Liu, C.-T. (1998). "Experimental study of drained creep behavior of sand." *J. Eng. Mech.*, 124(8), 912–920.

Lade, P. V., Nam, J., and Liggio, C. D., Jr. (2010). "Effects of particle crushing in stress drop-relaxation experiments on crushed coral sand." *J. Geotech. Geoenviron. Eng.*, 136(3), 500–509.

Lade, P. V., Yamamuro, J. A., and Bopp, P. A. (1996). "Significance of particle crushing in granular materials." *J. Geotech. Engrg.*, 122(4), 309–316.

Lee, K. L., and Farhoomand, I. (1967). "Compressibility and crushing of granular soils in anisotropic triaxial compression." *Can. Geotech. J.*, 4(1), 68–86.

Lemaitre, J., and Chaboche, J. L. (1990). *Mechanics of solid materials*, Cambridge University Press, Cambridge.

Liingaard, M., Augustesen, A., and Lade, P. V. (2004). "Characterization of models for time-dependent behavior of soils." *Int. J. Geomech.*, 4(3), 157–177.

Lobo-Guerrero, S., and Vallejo, L. E. (2005a). "Analysis of crushing of granular material under isotropic and biaxial stress conditions." *Soils Found.*, 45(4), 79–87.

Lobo-Guerrero, S., and Vallejo, L. E. (2005b). "Crushing of weak granular material: Experimental-numerical analyses." *Geotechnique*, 55(3), 245–249.

Marsal, R. J. (1967). "Large scale testing of rockfill materials." *J. Soil Mech. and Found. Div.*, 93(2), 27–43.

Matsushita, M., Tatsuoka, F. Koseki, J., Cazacliu, B., Benedetto, H., and Yasin, S. J. M. (1999). "Time effects on the pre-peak deformation properties of sands." *Pre-failure deformation characteristics of geomaterials*, M. Jamiolkowski, R. Lancelotta, and D. LoPresti, eds., Balkema, Rotterdam, The Netherlands, 681–689.

McDowell, G. R., and Bolton, M. D. (1998). "On the micromechanics of crushable aggregates." *Geotechnique*, 48(5), 667–679.

Nakata, Y., Hyde, A. F. L., Hyodo, M., and Murata, H. (1999). "A probabilistic approach to sand particle crushing in the triaxial test." *Geotechnique*, 49(5), 567–583.

Nakata, Y., Hyodo, M., Hyde, A. F. L., Kato, Y., and Murata, H. (2001a). "Microscopic particle crushing of sand subjected to high pressure and one-dimensional compression." *Soils Found.*, 41(1), 69–82.

Nakata, Y., Kato, Y., Hyodo, M., Hyde, A. F. L., and Murata, H. (2001b). "One-dimensional compression behaviour of uniformly graded sand

related to single particle crushing strength." *Soils Found.*, 41(2), 39–51.

Rűsch, H. (1960). "Researches toward a general flexural theory for structural concrete." *J. Am. Concr. Inst.*, 57(1), 1–28.

Santucci de Magistris, F., and Tatsuoka, F. (1999). "Time effects on the stress-strain behaviour of Metramo silty sand." *Prefailure deformation characteristics of geomaterials*, M. Jamiolkowski, R. Lancelotta, and D. LoPresti, eds., Balkema, Rotterdam, The Netherlands, 681–689.

Skempton, A. W. (1954). "The pore pressure coefficients A and B." *Geotechnique*, 4, 143–147.

Suklje, L. (1969). *Rheological aspects of soil mechanics*, Wiley, London.

Tang, C. A., Xu, X. H., Kou, S. Q., Lindqvist, P.-A., and Liu, H. Y. (2001). "Numerical investigation of particle breakage as applied to mechanical crushing. Part I: Single-particle breakage." *Int. J. Rock Mech. Min. Sci.*, 38, 1147–1162.

Tatsuoka, F., Enomoto, T., and Kiyota, T. (2006). "Viscous property of geomaterial in drained shear." *Geomechanics II—Testing, modeling and simulation*, Proc., 2nd Japan–U.S. Workshop, Vol. 156, P. V. Lade and T. Nakai, eds., ASCE, Kyoto, 285–312.

Tatsuoka, F., Santucci de Magistris, F., Hayano, K., Momoya, Y., and Koseki, J. (2000). "Some new aspects of time effects on the stress-strain behaviour of stiff geomaterials." *The geotechnics of hard soils—Soft rocks, 1998*, Vol. 2, R. Evangelista and L. Picarelli, eds., Balkema, Rotterdam, The Netherlands, 1285–1371.

Tatsuoka, F., Shihara, M., Di Benedetto, H., and Kuwano, R. (2002). "Time-dependent shear deformation characteristics of geomaterials and their simulation." *Soils Found.*, 42(2), 103–129.

Vallejo, L. E., Lobo-Guerrero, S., and Hammer, K. (2006). "Degradation of a granular base under a flexible pavement: DEM simulation." *Int. J. Geomech.*, 6(6), 435–439.

Yamamuro, J. A., Bopp, P. A., and Lade, P. V. (1996). "One-dimensional compression of sands at high pressures." *J. Geotech. Engrg.*, 122(2), 147–154.

Yamamuro, J. A., and Lade, P. V. (1993). "Effects of strain rate on instability of granular soils." *Geotech. Test. J.*, 16(3), 304–313.